Resonant suppression of Turing patterns by periodic illumination

Milos Dolnik,* Anatol M. Zhabotinsky, and Irving R. Epstein
Department of Chemistry and Volen Center for Complex Systems, Brandeis University, Waltham, Massachusetts 02454-9110
(Received 26 September 2000; published 12 January 2001)

We study the resonant behavior of Turing pattern suppression in a model of the chlorine dioxide-iodine-malonic acid reaction with periodic illumination. The results of simulations based on integration of partial differential equations display resonance at the frequency of autonomous oscillations in the corresponding well stirred system. The resonance in Turing pattern suppression is sharper at lower complexing agent concentration and is affected by the waveform of the periodic driving force. Square wave (on-off) periodic forcing is more effective in suppressing Turing patterns than sinusoidal forcing. We compare the dynamics of periodically forced Turing patterns with the dynamics of periodically forced nonhomogeneous states in a system of two identical coupled cells. Bifurcation analysis based on numerical continuation of the latter system gives good predictions for the boundaries of the major resonance regions of the periodically forced patterns.

DOI: 10.1103/PhysRevE.63.026101 PACS number(s): 82.40.Ck, 47.54.+r, 82.40.Bj

I. INTRODUCTION

Turing's work [1], published almost half a century ago, has had a profound impact on theoretical developments in pattern formation. Turing showed how spontaneous pattern formation may arise from the interaction of reaction and diffusion in a chemical system. Despite considerable efforts to experimentally verify Turing's idea and to find stationary spatial patterns in a real chemical system, it took almost 40 years before the first experimental evidence of convection-free Turing patterns was reported [2]. The Bordeaux group, working with an open continuously fed unstirred reactor (CFUR) observed spatial pattern formation arising from a homogeneous steady state in the chlorite-iodide-malonic acid (CIMA) reaction. Since then, Turing patterns have been extensively studied in the CIMA reaction and in its variant, the chlorine dioxide-iodine-malonic acid (CDIMA) reaction [3–5]. In recent years, increasing attention has been devoted to another, oscillatory class of Turing patterns, which arise through the wave instability [6]. Examples of oscillatory standing patterns include standing waves [7] and oscillatory clusters [8]. Despite the considerable interest and progress in the study of Turing patterns, little is known about their behavior in the presence of periodic external forcing.

Illumination and electric fields have been used to affect Turing-like patterns obtained during polymerization in the acrylamide-methylene blue-sulfide-oxygen reaction [9], and the same system has been exposed to spatially periodic light perturbation [10]. The pattern formation was modified by light, and both spatial synchronization with the perturbation and irregular responses were observed. The disadvantage of this system is its irreversibility; once the polymerization is over, the pattern cannot be changed by further external perturbation. This is not the case for the CIMA or CDIMA reaction in a CFUR, where patterns can be repeatedly exposed to external forcing. Recent experiments using the CDIMA reaction have revealed a sensitivity of this reaction to visible light [11,12] and opened the possibility of controlling Turing patterns by constant or periodic illumination. A further experimental study [13] revealed that spatially uniform illumination of Turing structures affects the characteristics of the patterns and, at larger intensities, eliminates pattern formation completely. When the light was periodically switched on and off, the fastest pattern suppression was observed at a frequency of illumination equal to the frequency of autonomous oscillations in the corresponding well stirred system. It was also found that periodic illumination is more effective than constant illumination with the same average light intensity.

Light is often used to study the effects of external perturbations on the dynamics of nonlinear reaction-diffusion systems. One of the most thoroughly studied systems is the photosensitive Belousov-Zhabotinsky (BZ) reaction with the $Ru(bpy)_3$ catalyst [14–16] immobilized in a thin layer of silica gel. Previous works have shown that traveling-wave patterns observed in this photosensitive BZ reaction may show spatial reorganization when subjected to periodic illumination. Resonant, frequency-locked regimes of standing-wave patterns were observed during periodic forcing of a rotating spiral wave [17,18]. The sequence of frequency-locked regimes is analogous to that of locked oscillations observed in a well mixed reactor [19].

Here, we study the resonant behavior of Turing structure suppression in a simple model of the CDIMA reaction with periodic illumination. We investigate how the waveform of the periodic driving force influences pattern suppression. We also compare the dynamics of periodically forced Turing patterns with the dynamics of a periodically forced system of two coupled identical cells. We demonstrate how a bifurcation analysis of the nonhomogeneous states in the system of two coupled cells can be used to predict the boundaries of the major resonance regions of the periodically forced patterns.

II. ILLUMINATION OF TURING PATTERNS WITH CONSTANT LIGHT

We employ the simplified two-variable model [20] modified to include the effect of illumination [11,13]:

*Author to whom correspondence should be addressed.

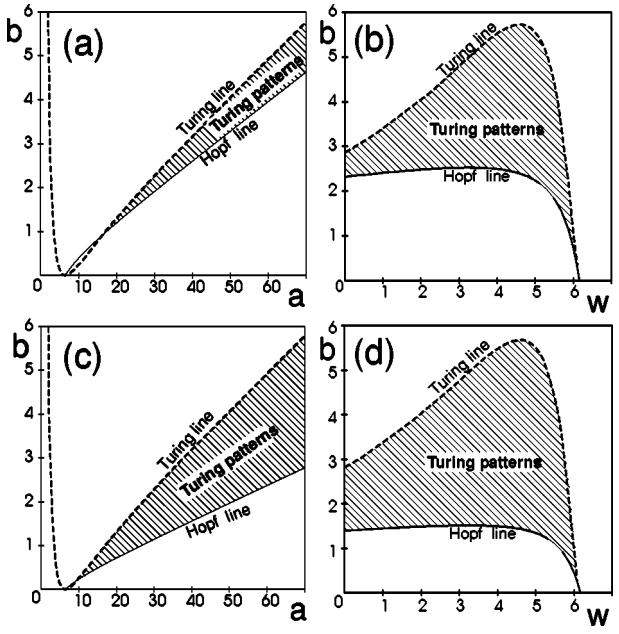

FIG. 1. Domains of Turing patterns in b vs a and b vs w parameter spaces in a model of the CDIMA reaction-diffusion system with constant illumination, Eq. (1). Parameters: (a) $\sigma=9$, $w=0$; (b) $\sigma=9$, $a=36$; (c) $\sigma=15$, $w=0$; (d) $\sigma=15$, $a=36$.

$$\frac{\partial u}{\partial t}=a-u-4\frac{uv}{1+u^2}-w+\nabla^2 u,$$

$$\frac{\partial v}{\partial t}=\sigma\left[b\left(u-\frac{uv}{1+u^2}+w\right)+d\nabla^2 v\right]. \qquad (1)$$

Here u and v are the dimensionless concentrations of $[I^-]$ and $[ClO_2^-]$, respectively; a and b are dimensionless parameters, with a proportional to the $[CH_2(COOH)_2]/[ClO_2]$ ratio and b to the $[I_2]/[ClO_2]$ ratio. Parameter d is equal to the ratio of diffusion coefficients $d=D_{ClO_2^-}/D_{I^-}$ and in this study it is fixed at the value $d=1.2$; σ depends on the complexing agent (starch) concentration according to $\sigma=1+K[I_2][S]$, where K is the association constant of the starch-triiodide complex and $[S]$ is the concentration of starch-triiodide binding sites [21]. Parameter w is the dimensionless rate of the photochemical reaction, which is proportional to the light intensity.

Figure 1(a) shows the region of existence of Turing patterns in the b vs a parametric space for $\sigma=9$. The Turing line is independent of the complexing agent concentration, but the position of the Hopf line varies with σ. Increasing the starch concentration shifts the Hopf line to lower values of b and thus increases the size of the Turing pattern region in the b vs a plane. The Hopf line lies above the Turing line for $a<17$, and no Turing patterns can be obtained below this value. When the CDIMA reaction-diffusion system is illuminated, i.e., $w>0$, both the Turing and Hopf lines are affected by the illumination. Figure 1(b) shows the Turing pattern region in the b vs w parameter plane. The Hopf line moves only slightly when the intensity of illumination is varied between 0 and 5. The changes in the Turing line are much larger within this range, which leads to an increase in the width of the Turing pattern region. When $w>5$, both the Turing and the Hopf bifurcations are strongly shifted to smaller values of b as the distance between these points shrinks. The Turing patterns cease to exist at an intensity of illumination slightly above $w=6$. In this case, a homogeneous stable steady state is reached.

Numerical integration of Eq. (1) in two-dimensional (2D) space reveals that some of the bifurcations are subcritical. Turing patterns are found for any initial condition in the region between the Hopf and Turing lines (Fig. 1). If stationary Turing patterns from previous runs are used as the initial conditions, then Turing patterns can also be obtained for certain parameters below the Hopf line (in the region of bulk oscillations) and above the Turing line (in the region of the uniform steady state). This observation indicates that both the Hopf and the Turing bifurcations can be subcritical, which leads to bistability between the Turing patterns and the homogeneous steady state, and between the Turing patterns and the bulk oscillations. Similar subcritical transitions to Turing patterns have been reported earlier [5,22]. Figure 2 displays patterns obtained for different values of b and w using Turing patterns as initial conditions. The thick lines in

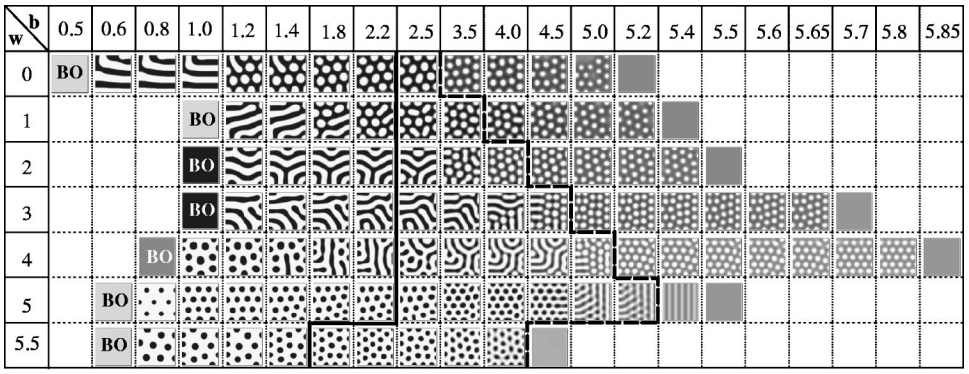

FIG. 2. Turing patterns in a model of the CDIMA reaction-diffusion system with constant illumination. Turing patterns at higher values of b are surrounded by a uniform homogeneous state and at lower b by homogeneous bulk oscillation (BO). Columns in the table illustrate transformation of Turing patterns when illumination intensity is varied. Parameters: $\sigma=9$, $a=36$. Thick solid line: Hopf bifurcation line; thick dashed line: Turing line.

Fig. 2, which correspond to the Turing and Hopf lines, indicate the boundaries of the Turing pattern region. Figure 2 illustrates that the Turing pattern can be modified not only by varying the input concentrations (parameter b) but also by changing the intensity of uniform illumination. For example, when b is fixed at 2.5 and w is gradually increased, the Turing pattern changes from hexagons to mixed hexagons and stripes, stripes, stripes-honeycombs, and pure honeycombs before stronger illumination leads to total suppression of Turing patterns.

III. PERIODIC ILLUMINATION OF TURING PATTERNS

In a previous experimental study [13], we observed that periodic illumination is more effective in suppressing Turing patterns than constant illumination with the same average light intensity. The experiments show the fastest suppression of pattern formation at a frequency of illumination equal to the frequency of autonomous oscillations in the corresponding well stirred system. Numerical simulations displayed similar resonant behavior of periodically illuminated Turing patterns. Here, we extend our numerical study of periodic illumination of Turing patterns and analyze the resonant dynamics of Turing pattern suppression. We employ both square-wave (on-off) and sinusoidal-wave forms for the periodic light signal. In all simulations with periodic illumination we fix the parameters at $a=36$ and $b=2.5$ and vary the period of illumination T and the maximum light intensity W.

Square-wave illumination. Square-wave illumination was used in the experiments described in Ref. [13]. The light is periodically switched on and off with equal durations of the *on* and *off* phases. The light intensity w is a periodic function of time:

$$w(t)=W \quad \text{for} \quad iT \leqslant t < iT+T/2,$$
$$w(t)=0 \quad \text{for} \quad iT+T/2 \leqslant t < (i+1)T. \tag{2}$$

Here $i=0,1,2,\ldots$ and T is the period of illumination.

Sinusoidal-wave illumination. To study the role of the perturbation waveform in resonant behavior we also employ sinusoidal-wave illumination, which is a periodic function of time according to

$$w(t)=\frac{W}{2}\left[1+\sin\left(\frac{2\pi t}{T}\right)\right]. \tag{3}$$

The term $w(t)$ is always nonnegative, and the time-averaged intensity over an integer number of periods is the same for the same maximum intensity W in the case of sinusoidal- and square-wave illumination.

Figure 3 compares the results of simulations for square- and sinusoidal-wave illumination for two values of σ. The line divides the amplitude-period parameter space into two regions. When the parameters lie in the region above the solid (dashed) line for $\sigma=9$ ($\sigma=15$), periodic forcing results in total suppression of Turing patterns. A spatially uniform state replaces the Turing patterns after a transient period and, if the periodic illumination is continued after

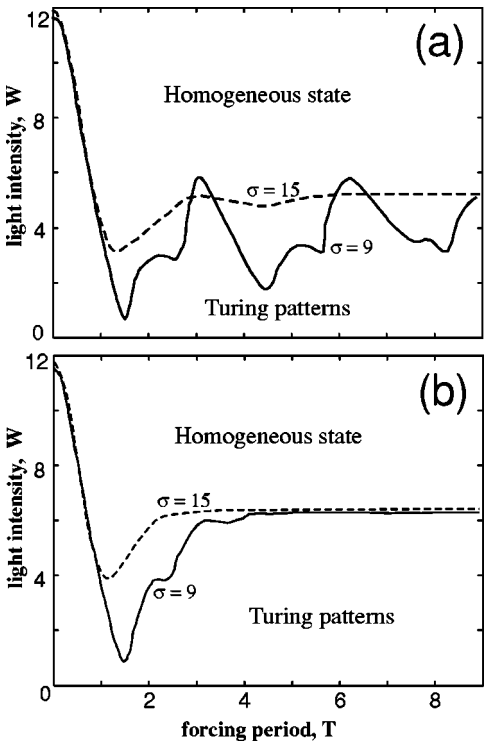

FIG. 3. Resonant dynamics of periodically forced Turing patterns in a 2D system according to Eq. (1). The boundary between the domain of the Turing patterns and that of the spatially homogeneous state is calculated for $\sigma=9$ (solid line) and 15 (dashed line). Other parameters are $a=36$, $b=2.5$. (a) Square-wave (on-off) illumination. (b) Sinusoidal-wave illumination.

Turing structure suppression, periodic bulk oscillations of the whole medium ensue. The frequency of these bulk oscillations is synchronized with the frequency of illumination. If the periodic illumination ceases during or after pattern suppression, the Turing patterns reappear, because they are the only stable solution in the absence of light for the parameters in Fig. 3 [see Fig. 1(b)].

The solid line in Fig. 3(a) for $\sigma=9$ shows strong resonances in the suppression of Turing patterns with numerous local minima and maxima for square-wave illumination. The global minimum is located near period $T=1.55$, which almost coincides with the period of oscillations of the starch-free system ($\sigma=1$). If this frequency is used for illumination, then light of maximum intensity $W=0.6$ is enough to eliminate the pattern. This value is approximately 20 times less than the average intensity required when using constant illumination. Other local minima are found near odd multiples of this period (odd subharmonics) at $T=4.6$ and 7.7. On the other hand, the even subharmonics display antiresonance behavior—near $T=3.1$ and $T=6.2$ maximal intensity is required to suppress pattern formation.

With sinusoidal- instead of square-wave illumination, the major resonance is found for the same period [solid lines in Figs. 3(a) and 3(b)], but the subharmonic resonance nearly vanishes, and for $T>3$ the minimum light intensity required to suppress the pattern is practically independent of frequency.

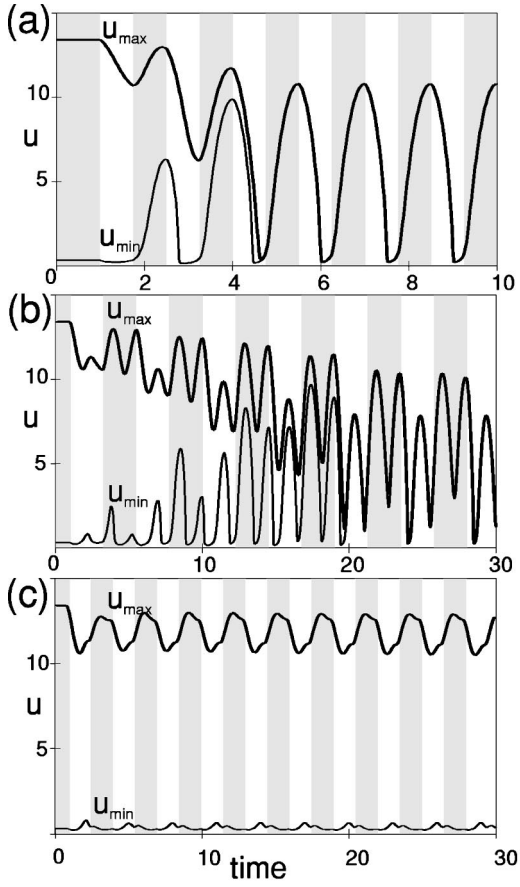

FIG. 4. Periodic square-wave illumination of Turing patterns—temporal profiles of maximum and minimum values of u. (a) Period of illumination $T=1.5$, resonance 1:1 with suppression of Turing patterns within three periods of illumination. (b) $T=4.5$, resonance 3:1 with suppression of Turing patterns within five periods of illumination. (c) $T=3.0$, antiresonance 2:1 with no suppression of Turing patterns. Parameters: $w=2$, other parameters as in Fig. 3.

At higher concentrations of the complexing agent ($\sigma=15$) the minimum intensity required for pattern suppression at the resonant frequency is almost 10 times larger than at $\sigma=9$. For $\sigma=15$, resonant suppression is found only near the frequency of damped oscillations in a diffusion-free system. The curve that separates the Turing patterns from the homogeneous state displays a minimum at roughly three times the basic period for square-wave illumination, but this minimum is much shallower than for $\sigma=9$. Only a single minimum (resonance) is found for sinusoidal-wave illumination. Square-wave illumination is more effective than sinusoidal both for $\sigma=9$ and $\sigma=15$, as shown by the fact that the amplitude of square-wave illumination required to suppress Turing patterns at a given period is less than or equal to the corresponding sinusoidal illumination amplitude.

Figure 4 illustrates the process of Turing pattern suppression. The time-dependent behavior during square-wave illumination is shown at two points selected from a 2D Turing pattern. The thick line depicts the concentration changes at a point where the pattern has its maximum concentration u_{max}; the thin line shows the changes at a point with minimum concentration u_{min}. Gray and white backgrounds indicate the light intensity; white corresponds to the light being on. Increasing the illumination intensity decreases the iodide concentration [11]. Our simulations show that for the low concentration of complexing agent $\sigma\leqslant 15$, a change in the intensity of illumination is followed by damped oscillations. Thus, the changes in I^- induced by illumination interact with the damped oscillatory adaptation of the Turing pattern to a new light level. If the illumination varies at the frequency of the damped oscillations, then u_{min} and u_{max} approach each other, and their merging leads to Turing pattern suppression. Figure 4(a) displays an example of such pattern suppression. At time $t=1$, immediately after the light is switched on, both u_{min} and u_{max} decrease. After half a period of illumination, at $t=1.75$, u starts to rise again as a result of the damped oscillations. At the same time, the light is switched off and the rise in u is enhanced by the decrease in illumination. Although there is significant change in both u_{min} and u_{max}, one can see a more profound increase in the former concentration. After another half period, when the light is switched on again, the decrease in u caused by illumination remains in synchrony with the damped oscillations, leading to a strong decrease in both u_{min} and u_{max}. Over several cycles, the minimum and maximum values of u approach each other. Once they merge, the Turing pattern disappears. Figure 4(b) shows a similar record for an illumination period three times as long as that in Fig. 4(a). In this case, there is 3:1 entrainment between the period of damped oscillation and the period of illumination. It takes more cycles than in Fig. 4(a) to bring the minimum and maximum together for full suppression of patterns in this case. On the other hand, when we use a period of illumination that is double the period of damped oscillation, the rises and falls in u and the damped oscillations are out of phase. The light is switched off when u reaches its local maximum and switched on when u reached its local minimum. Thus, the concentration changes resulting from illumination counterbalance the damping changes, and we do not obtain the large deviations in u_{min} and u_{max} that would lead to pattern suppression. This analysis suggests why at illumination periods equal to even multiples of the damping period we observe antiresonance behavior [see Fig. 4(c)].

IV. BIFURCATION ANALYSIS OF A TWO-CELL SYSTEM WITH CONSTANT ILLUMINATION

The determination of boundaries for Turing pattern suppression as shown in Fig. 3 directly by integration of partial differential equations (PDE's) in two dimensions is a time-consuming task. A reaction-diffusion system is described by a system of parabolic PDE's, which are numerically solved by a finite difference method that converts the PDE's into a set of ordinary differential equations (ODE's) using a discrete set of spatial points with equidistant grid spacing. As an alternative to direct integration, one might attempt to study the stability of the steady states and periodic solutions of the ODE's, using continuation algorithms [23,24]. Though numerical continuation packages provide a powerful tool for these studies, the number of ODE's arising from the finite

difference method is too large to be handled by currently available packages.

The diffusion-induced instability that leads to the formation of spatial stationary patterns can also occur in a system of two homogeneous cells coupled by diffusion [1]. This system represents the minimal configuration for diffusion-induced instability and can be viewed as the smallest unit that can be obtained from a set of PDE's by the finite difference method. Several studies of such systems have been performed in the past, many of them with Brusselator kinetics [21,25–27].

Here we consider a system of two identical cells containing the components of the CDIMA reaction, including starch, and linked by diffusion coupling. Such systems can be built from two well stirred reactors connected by a common wall via a semipermeable membrane, through which the chemicals diffuse according to Fickian diffusion.

Our system is then described by the following set of equations:

$$\frac{du_1}{dt} = a - u_1 - 4\frac{u_1 v_1}{1+u_1^2} - w + u_2 - u_1,$$

$$\frac{dv_1}{dt} = \sigma\left[b\left(u_1 - \frac{u_1 v_1}{1+u_1^2} + w \right) + d(v_2 - v_1) \right],$$

$$\frac{du_2}{dt} = a - u_2 - 4\frac{u_2 v_2}{1+u_2^2} - w + u_1 - u_2,$$

$$\frac{dv_2}{dt} = \sigma\left[b\left(u_2 - \frac{u_2 v_2}{1+u_2^2} + w \right) + d(v_1 - v_2) \right]. \qquad (4)$$

To find the steady state and periodic solutions of Eq. (4) and to determine their stability, we use the program package CONT [28]. We first calculate the solution diagrams as the dependents of the steady state values in cell 1, u_1, and in cell 2, u_2 on a single parameter (a, b, or w).

The steady state solution diagrams display branches with a stable homogeneous steady state (HS), in which $u_1 = u_2$ and $v_1 = v_2$. HS becomes unstable either at a Hopf bifurcation point, where an oscillatory solution emerges, or at a branching (pitchfork) bifurcation point, where nonhomogeneous steady state solutions (NS) with $u_1 \neq u_2$ and $v_1 \neq v_2$ arise. The oscillatory solutions are found to be homogeneous (HO) or nonhomogeneous (NO), and their stability is determined from Floquet multipliers [23]. Bifurcation points from the solution diagrams are used as starting points to calculate the bifurcation lines for construction of two-parameter bifurcation diagrams. We compare these diagrams with those obtained for the full reaction-diffusion system (see Fig. 1).

Figure 5 contains the solution diagram, which shows dependence of variables u_1 and u_2 on parameter a for fixed $b = 2.5$ and $\sigma = 15$. The diagram is shown together with examples of the dynamical behavior at six selected points. One stable HS is found for $a < 40.75$ (point A). At the branching (pitchfork) point ($a = 40.75$) HS becomes unstable (dotted line) and two NS's emerge. At the subcritical Hopf bifurcation point at $a = 41.70$ the NS becomes unstable. At the Hopf bifurcation point a branch of unstable periodic solutions (NO type) emerges, which is shown in Fig. 5 with open circles. The minima and maxima of u_1 and u_2 are shown along the branches of periodic solutions. At $a = 40.78$ there is a limit point of periodic solutions, where a branch of periodic solutions changes stability and becomes stable (filled circles). Therefore, at point B ($a = 41.0$) we find two stable nonhomogeneous solutions—NO and NS. At point C ($a = 45.0$), which is beyond the Hopf bifurcation point, the NO state is the only stable solution.

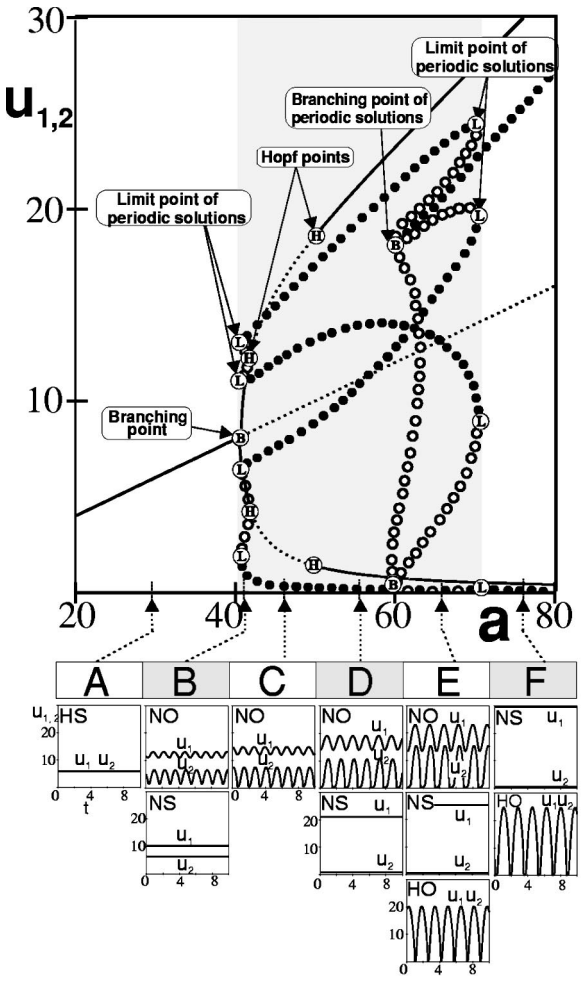

FIG. 5. System of two coupled cells with a CDIMA reaction. Solution diagram and examples of stable regimes at selected values of parameter a. Points: A, $a = 30.0$, only homogeneous steady state (HS) is stable; B, $a = 41.0$, nonhomogeneous oscillation (NO) coexists with nonhomogeneous steady state (NS); C, $a = 45.0$, only NO is stable, D, $a = 55.0$, NO and NS coexist; E, $a = 65.0$, NO, NS, and homogeneous oscillations (HO) coexist; F, $a = 75.0$, NS and HO coexist. Gray shading in the solution diagram indicates the region between limit points of nonhomogeneous period solutions, where nonhomogeneous oscillations are stable.

At $a = 50.50$, there is another subcritical bifurcation on the NS branch (the unstable branch of periodic solutions emerging from this Hopf point is not shown in Fig. 5) and the NS becomes stable again. Thus, at point D we obtain the same set of dynamical behaviors as at point B. The branch of

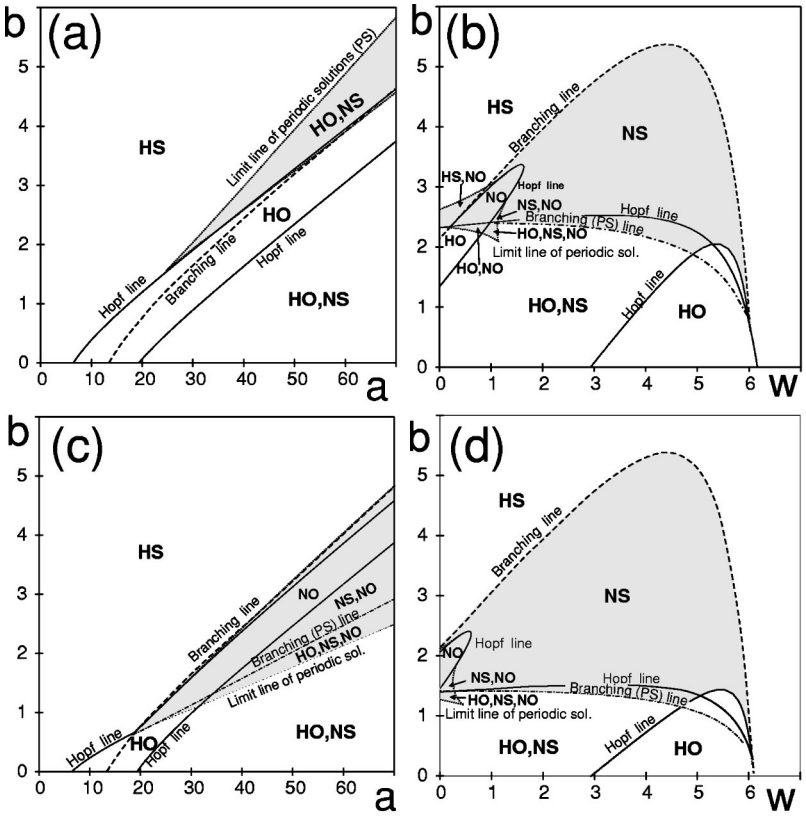

FIG. 6. System of two coupled cells with a CDIMA reaction—two-parameter bifurcation diagrams. Parameters are analogous to those used in Fig. 1. (a) $\sigma=9$, $w=0$; (b) $\sigma=9$, $a=36$; (c) $\sigma=15$, $w=0$; (d) $\sigma=15$, $a=36$. Gray areas in diagram are regions with stable nonhomogeneous oscillations, and regions where only nonhomogeneous steady states are stable.

nonhomogeneous periodic solutions undergoes another limit point bifurcation at $a=70.24$ and then ends at a branching point of periodic solutions where $a=60.28$. At this point, the stable homogeneous oscillations emerge. Thus, for a between 60.28 and 70.24 we obtain three stable solutions (point E)—two nonhomogeneous (NO and NS) and one homogeneous (HO). For $a>70.24$, HO coexists with NS (point F).

We further use the bifurcation points from the one-parameter solution diagrams and perform continuation of these points to obtain two-parameter bifurcation diagrams. The results of these continuations are summarized in Fig. 6 for $\sigma=9$ and 15. Comparing Fig. 6 with Fig. 1, one can see that the NO regions, together with the region where only NS is stable in the system of two coupled cells (gray shaded area), correlate with the Turing pattern regions (hatched area) for the reaction-diffusion system. With increasing complexing agent concentration the area of this region increases in a similar fashion in both cases. Thus, a system of two coupled cells provides a good model for the full reaction-diffusion system.

V. PERIODIC ILLUMINATION OF TWO COUPLED CELLS

The resonance behavior and parameter dependences of resonant periodic orbits and their bifurcations have been studied for many years [27,29–31]. We further utilize the software package CONT for the continuation of periodically forced ODE's to investigate bifurcations in the system of two coupled identical cells described by Eq. (4), with w as a periodic function of time in both cells. We employ both square-wave and sinusoidal-wave illumination according to Eq. (2) and Eq. (3).

A. Bifurcation of periodic solutions and Turing patterns

Figure 7 shows a diagram for period-one solutions in a system of two coupled cells with sinusoidal illumination at a fixed period of illumination $T=2$. For $W<0.331$ the homogeneous period-one solution is stable and coexists with nonhomogeneous (complex) oscillation, which results from a subcritical torus bifurcation of the nonhomogeneous periodic solution at $W=0.336$. At $W=0.615$ there is a supercritical torus bifurcation, which means that for $W>0.615$ the nonhomogeneous period-one oscillations are stable. These oscillations again become unstable at a limit point ($W=1.654$), and the branches of nonhomogeneous periodic solutions terminate at a branching point at $W=1.644$. For $W>1.654$ we find only stable homogeneous oscillations. In the preceding section we showed that the region of Turing structures in the reaction-diffusion system correlates with the regions with stable nonhomogeneous states in the system of two coupled cells. Here we speculate that the parameter range in which nonhomogeneous states are stable (shaded area) corresponds to amplitudes of sinusoidal forcing that do not lead to suppression of Turing patterns in the reaction-diffusion system. We further calculate the dependences of the bifurcation points on the amplitude and period of forcing in order to obtain a resonance diagram of homogeneous and nonhomogeneous solutions. Figure 8 displays the branching, limit, torus, and period doubling lines for the period-one solution. The limit lines for $W<1$ show the boundaries of the resonant

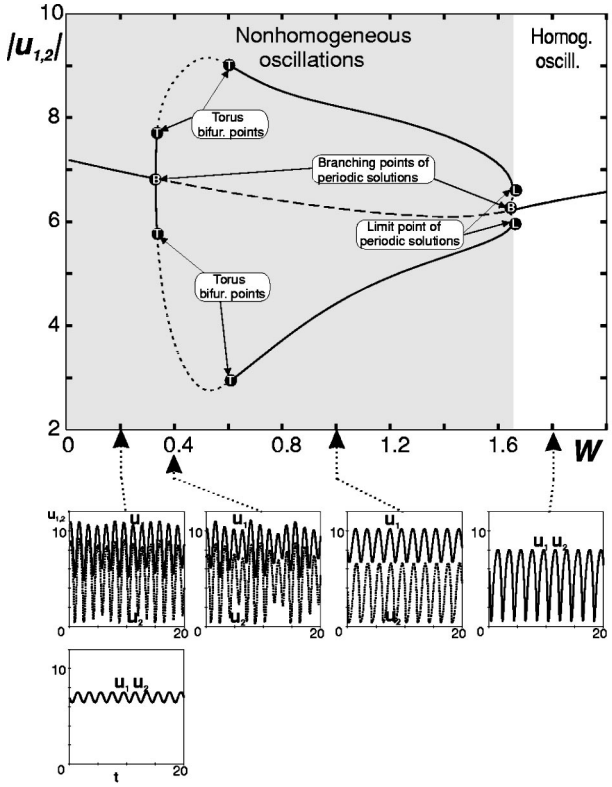

FIG. 7. Two coupled cells with sinusoidal periodic illumination—period-one solutions. Parameters: $T=2.0$, $\sigma=9$, $b=2.5$, $a=36$. Region of nonhomogeneous oscillations is gray. Solid line represents stable, period-one, homogenous (HO) and nonhomogeneous (NO) oscillations; dashed line represents unstable HO, dotted line unstable NO. Examples of stable solutions at several amplitude values of illumination are shown at the bottom.

regions (Arnol'd tongues), which originate on the T axis ($W=0$) at $T\approx 1.6$, 3.2, 4.8, and 6.4. The torus and period doubling lines lie between the resonant regions. Inside the resonant regions there are stable period-one nonhomogeneous solutions, while outside these regions complex nonhomogeneous periodic solutions can be found. These complex periodic solutions arise via torus or period doubling bifurcations. From the assumption that the region of stable nonhomogeneous periodic solutions is associated with the Turing pattern region, we relate the topmost supercritical branching bifurcation line or (in the case of subcritical bifurcation) the limit line of periodic solutions to the boundary of Turing pattern suppression. In Fig. 9 we overlay these bifurcation lines with the boundary detected by direct integration of the two-dimensional reaction-diffusion system [Eq. (1)]. The agreement between the region of nonhomogeneous solutions in the two-cell system with the region of Turing patterns in the reaction-diffusion system is very good. The initial conditions used in our direct integration are the same in all runs—a stationary Turing pattern. We have performed several runs with other initial conditions and found that Turing patterns can be suppressed for amplitudes between the limit line and the subcritical branching line, which indicates a region of coexistence of Turing patterns with the uniform state.

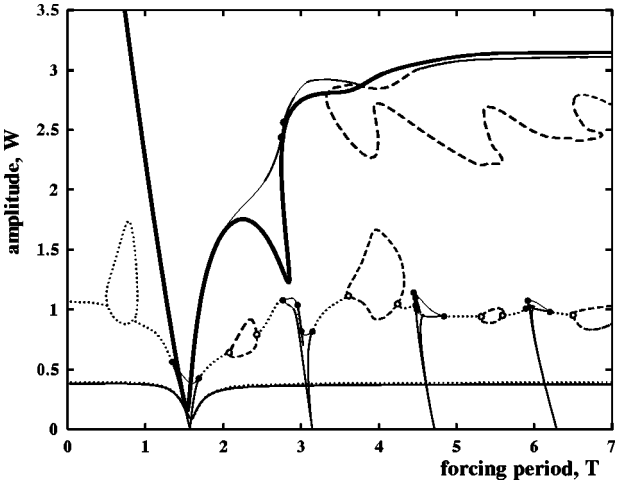

FIG. 8. Resonance regions in two coupled cells with periodic sinusoidal-wave illumination. Thick solid line, line of branching points of HO; thin solid line, line of limit points of NO; dashed line, period doubling line of NO; dotted line, line of torus bifurcation points. Solid circles, Takens-Bogdanov points; open circle, degenerate period doubling points. $\sigma=9$, $a=36$, $b=2.5$.

B. Resonant dynamics of two coupled cells with periodic illumination

Figure 3, which shows resonance in the suppression of Turing patterns by periodic illumination, illustrates the effects of the waveform of periodic illumination and of the complexing agent concentration. The resonant dynamics obtained from continuation of periodic solutions in a system of two coupled cells displays similar features. Figure 10 shows the branching and limit lines for three different shapes of

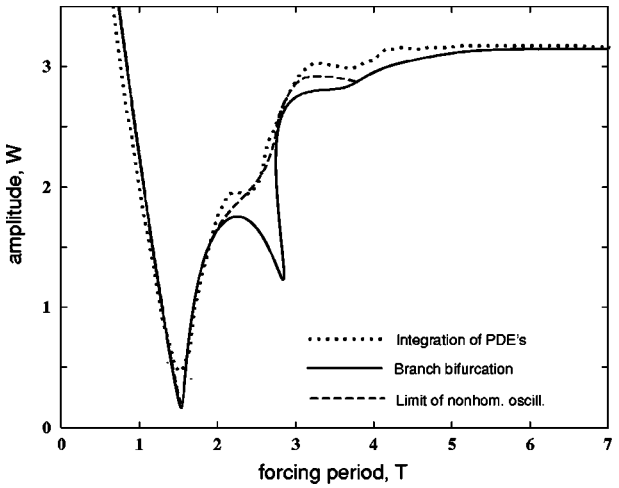

FIG. 9. Comparison of resonance in the suppression of Turing patterns in a reaction-diffusion system and in the suppression of nonhomogeneous states in a system of two coupled cells. Sinusoidal waveform for $\sigma=9$, $a=36$, $b=2.5$. The dotted line shows the boundary of Turing pattern suppression obtained from direct simulations of Eq. (1). The thick solid line is the line of branching points of HO and the thin solid line is the line of limit points of NO for system of two coupled cells with a CDIMA reaction. Parameters as in Fig. 8.

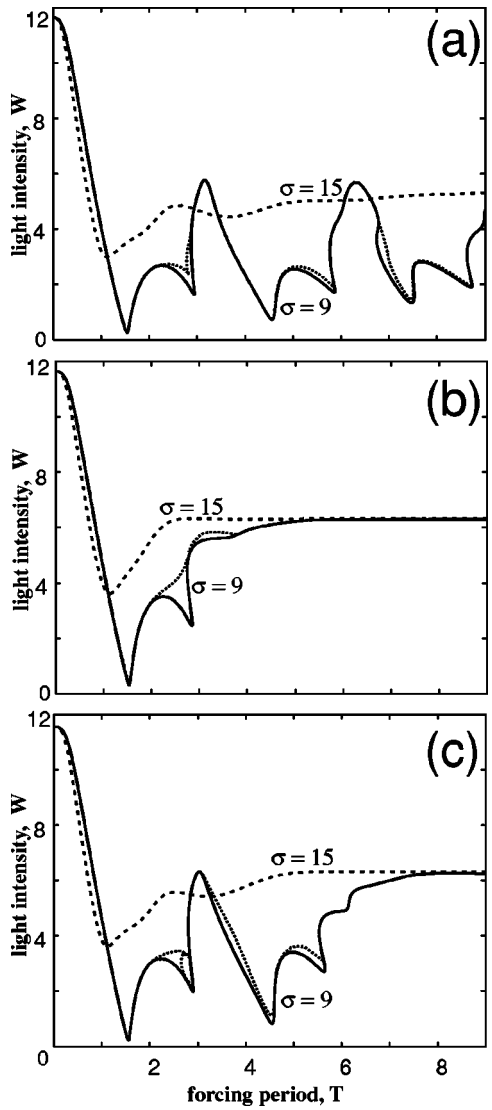

FIG. 10. Resonance in the suppression of nonhomogeneous states; dependence on the illumination waveform for $\sigma=9$ and $\sigma=15$. (a) Square (on-off) waveform. (b) Simple sinusoidal waveform. (c) Sinusoidal waveform composed of the first two terms of the Fourier series of square waves. For $\sigma=9$, when the branching bifurcation of periodic solutions (solid line) is subcritical, the line of limit points (dotted line) marks the boundary of nonhomogeneous oscillations. For $\sigma=15$, the branching bifurcation (dashed line) is always supercritical.

periodic illumination. Figure 10(a) shows that for square-wave illumination and $\sigma=9$ the bifurcation lines display resonant periods with a major resonance at $T\approx1.55$ (close to the period of damped oscillations) and its odd subharmonics. Some resonance behavior also occurs near even subharmonics ($T\approx3.1,6.2,\ldots$), but these minima are much shallower and are rapidly followed by antiresonant behavior (maxima). Simulations with $\sigma=15$ display much less pronounced resonance behavior. The only minima on the bifurcation line occur at the fundamental period and at triple that value. Figure 10(b) shows the results of continuation for sinusoidal-wave illumination. The resonance occurs only around the period of damped oscillations both for $\sigma=9$ and $\sigma=15$. Here, too, a larger value of σ results in a shallower resonance domain. Comparison of the border of Turing pattern suppression (Fig. 3) and the branching and/or limit bifurcation lines (Fig. 10) gives almost quantitative agreement for both square-wave and sinusoidal-wave illumination.

We also performed simulations with a waveform composed of the first two harmonics from the Fourier transform of the square wave. The square-wave illumination can be written in the form of an infinite Fourier series

$$w(t)=\frac{W}{2}\left(1+\sin\frac{2\pi t}{T}+\frac{1}{3}\sin\frac{6\pi t}{T}+\frac{1}{5}\sin\frac{10\pi t}{T}+\cdots\right). \tag{5}$$

We employed a combination of two sinusoidal waves:

$$w(t)=\frac{W}{2}\left(1+\sin\frac{2\pi t}{T}+\frac{1}{3}\sin\frac{6\pi t}{T}\right). \tag{6}$$

Figure 10(c) shows the bifurcation lines with resonances at the basic and triple periods of damped oscillations.

C. Resonance in a modified model for illumination of the CDIMA reaction

In a recent study, a new mechanism for determining the effect of visible light on the CDIMA reaction was proposed [12]. In this model, the overall rate of the light-sensitive part of the mechanism depends on $[ClO_2]$ and $[I^-]$ as well as on the light intensity. In the simplified two-variable version, Eq. (7), $[ClO_2]$ is considered constant, and we replace w in Eq. (1) with

$$w=\frac{\alpha w'}{u+c}. \tag{7}$$

Here, w' is proportional to the light intensity and c and α are constants. Figure 11(a) shows a bifurcation diagram in the b vs w' parameter space with Turing and Hopf lines for $c=0.8$ and $\alpha=2.5$. Comparing Fig. 11(a) with Figs. 1(b) and 1(d), we see that for $w'<4.5$ there is no significant change in the size and shape of the Turing pattern region. Only for larger values of the light intensity ($w'>4.5$) is the shape of the Turing and Hopf lines altered. Now Turing patterns are predicted to exist for very large values of parameter b, which does not occur when w is considered to be independent of $[ClO_2]$ and $[I^-]$. Figure 11(b) shows the line of branching bifurcations, which, as demonstrated in the preceding section, corresponds to the boundary of Turing pattern suppression in the reaction-diffusion system with periodic forcing. The periodic force in this case has the form

$$w_i(t)=\frac{\alpha w'}{2(u_i+c)}\left[1+\sin\left(\frac{2\pi t}{T}\right)\right], \tag{8}$$

where $i=1,2$. Owing to the dependence of the periodic forcing on the variables u_i, the forcing term is different in each cell in the case of the nonhomogeneous state. This feature

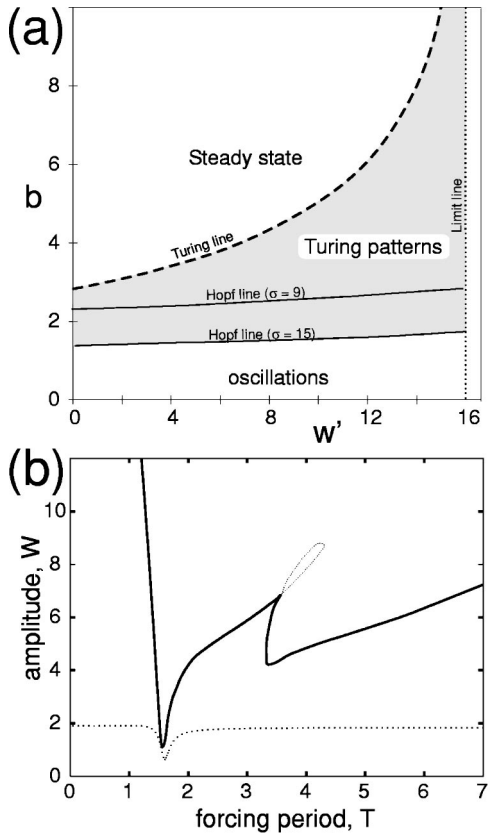

FIG. 11. Turing pattern domains in a modified model of the CDIMA reaction—Eq. (7). (a) Domains of Turing patterns in b vs W parameter space for a CDIMA reaction-diffusion system. (b) Resonance in the suppression of nonhomogeneous states in a system of two coupled cells, $\sigma=9$, sinusoidal illumination.

results in numerical difficulties in the continuation technique, which often fails to converge. Nevertheless, the resonance behavior is analogous to that obtained with a concentration-independent forcing term.

VI. DISCUSSION AND CONCLUSION

In this numerical study of the CDIMA reaction, we have analyzed resonant behavior during suppression of Turing patterns by periodic illumination. The resonant behavior is found to be more profound for lower starch concentrations and to vanish at high starch concentrations. Simulations show that for low starch concentrations the recovery to a steady state after a single perturbation exhibits well defined damped oscillations. At larger starch concentrations the damping becomes very strong, and for $\sigma \gg 15$ there is a fast nonoscillatory recovery to the steady state after perturbation. The interaction between the damped oscillations and periodic illumination is responsible for the observed resonances. The resonance in Turing pattern suppression is observed for a frequency which is close to the frequency of damped oscillations or which is an odd subharmonic of this frequency. Forcing with a period that is an even multiple of the period of damped oscillations yields antiresonant behavior. This behavior is caused by the opposing effects of the periodic forcing and the damped oscillations, which prevents suppression of the concentration gradient in the pattern.

The resonant behavior is affected by the waveform of the periodic illumination. Square-wave forcing is more effective in suppression of Turing patterns than a smooth sinusoidal waveform. We have performed a study with unequal on-off duration for rectangular waveform illumination. We find that for $T=1.55$ the ratio $t_{on}/t_{off}=1$ is the most effective for suppression of the patterns, i.e., the lowest intensity of illumination is needed at this ratio to suppress the Turing pattern. Similar results were obtained for $T=4.65$, where the most effective ratio was $t_{on}/t_{off}=0.9$. On the other hand, for $T=3.1$ the most effective ratios are found to be 0.25 and 4, while a ratio close to 1.5 gives a local minimum (maximum) in the effectiveness (intensity of illumination).

There is a simple relationship between the shape of the periodic forcing function and the resonant dynamics of Turing pattern suppression. At lower complexing agent concentrations ($\sigma=9$) resonance occurs at odd subharmonics. Simple sinusoidal forcing gives resonance at the basic frequency of damped oscillations; square-wave forcing, which is an infinite series of odd sinusoidal terms, results in resonance at the odd frequencies. A waveform consisting of only the first two terms from the Fourier series of a square wave results in a resonance structure almost identical to the resonances found in square-wave forcing at the fundamental and third subharmonics, but does not contain any further subharmonic resonances.

Our simulations confirm that periodic illumination is more effective than constant illumination. For example, at $\sigma=9$ the intensity of illumination needed to suppress the Turing pattern using square-wave illumination is only 5% of that required with constant illumination.

We have compared the dynamics of periodically forced Turing patterns with the dynamics of periodically forced nonhomogeneous states in a system of two coupled identical cells. Bifurcation analysis based on numerical continuation of the latter system gives very good predictions for the boundaries of the major resonance regions of periodically forced patterns. The results of simulations suggest that the regions of stable nonhomogeneous solutions in the system of two coupled cells are associated with the Turing pattern region in the continuous system. In the amplitude vs forcing period parameter plane, the topmost supercritical branching bifurcation line or (in the case of subcritical bifurcation) the limit line of periodic solutions corresponds closely to the boundary of Turing pattern suppression. The boundary in most cases does not deviate from the bifurcation lines by more than 5% of W and in the case of subcritical branching bifurcations, the boundary closely follows the limit line.

ACKNOWLEDGMENTS

This work was supported by the National Science Foundation. We thank Igor Schreiber for providing us with the most recent version of the CONT package.

[1] A. M. Turing, Philos. Trans. R. Soc. London, Ser. B **237**, 37 (1952).
[2] V. Castets, *et al.*, Phys. Rev. Lett. **64**, 2953 (1990).
[3] Q. Ouyang and H. L. Swinney, Nature (London) **352**, 610 (1991).
[4] I. Lengyel and I. R. Epstein, Accounts Chem. Res. **26**, 235 (1993).
[5] B. Rudovics *et al.*, J. Phys. Chem. A **103**, 1790 (1999).
[6] A. M. Zhabotinsky, M. Dolnik, and I. R. Epstein, J. Chem. Phys. **103**, 10 306 (1995).
[7] V. Petrov *et al.*, J. Phys. Chem. **100**, 18 992 (1996).
[8] V. K. Vanag *et al.*, Nature (London) **406**, 389 (2000).
[9] M. Watzl and A. F. Münster, J. Phys. Chem. **102**, 2540 (1998).
[10] F. Fecher *et al.*, Chem. Phys. Lett. **313**, 205 (1999).
[11] A. P. Munuzuri *et al.*, J. Am. Chem. Soc. **121**, 8065 (1999).
[12] A. K. Horvath *et al.*, J. Phys. Chem. A **104**, 5766 (2000).
[13] A. K. Horvath *et al.*, Phys. Rev. Lett. **83**, 2950 (1999).
[14] L. Kuhnert, K. I. Agladze, and V. I. Krinsky, Nature (London) **337**, 244 (1989).
[15] O. Steinbock, V. Zykov, and S. C. Muller, Nature (London) **366**, 322 (1993).
[16] S. Kadar, T. Amemiya, and K. Showalter, J. Phys. Chem. A **101**, 8200 (1997).
[17] V. Petrov, Q. Ouyang, and H. L. Swinney, Nature (London) **388**, 655 (1997).
[18] A. L. Lin *et al.*, Phys. Rev. Lett. **84**, 4240 (2000).
[19] M. Dolnik *et al.*, J. Phys. Chem. **93**, 2764 (1989).
[20] I. Lengyel and I. R. Epstein, Science **251**, 650 (1991).
[21] I. Lengyel and I. R. Epstein, Chaos **1**, 69 (1991).
[22] O. Jensen *et al.*, Phys. Lett. A **179**, 91 (1993).
[23] M. Kubicek and M. Marek, *Computational Methods in Bifurcation Theory and Dissipative Structures* (Springer, Berlin, 1983).
[24] E. J. Doedel and J. P. Kernevez, *AUTO: Software for Continuation and Bifurcation Problems in Ordinary Differential Equations* (California Institute of Technology, Pasadena, 1986).
[25] I. Prigogine and R. Lefever, J. Chem. Phys. **48**, 1695 (1968).
[26] J. J. Tyson and S. Kauffman, J. Math. Biol. **1**, 289 (1975).
[27] I. Schreiber *et al.*, J. Stat. Phys. **43**, 489 (1986).
[28] M. Marek and I. Schreiber, *Chaotic Behavior of Deterministic Dissipative Systems* (Cambridge University Press, Cambridge, 1991).
[29] L. Glass and R. Perez, Phys. Rev. Lett. **48**, 1772 (1982).
[30] K. Tomita, Phys. Rep. **86**, 113 (1982).
[31] I. G. Kevrekidis, R. Aris, and L. D. Schmidt, Chem. Eng. Sci. **41**, 1549 (1986).